PCCP

Accepted Manuscript

This is an *Accepted Manuscript*, which has been through the Royal Society of Chemistry peer review process and has been accepted for publication.

Accepted Manuscripts are published online shortly after acceptance, before technical editing, formatting and proof reading. Using this free service, authors can make their results available to the community, in citable form, before we publish the edited article. We will replace this *Accepted Manuscript* with the edited and formatted *Advance Article* as soon as it is available.

You can find more information about *Accepted Manuscripts* in the Information for Authors.

ROYAL SOCIETY OF CHEMISTRY

www.rsc.org/pccp

Journal Name

ARTICLE TYPE

Model of Ultra-Fast Charge Transport in Membrane Proteins

Sheh-Yi Sheu[a,*], Edward W. Schlag[b], and Dah-Yen Yang[c,*]

5 Isolated proteins have recently been observed to transport charge and reactivity over very long distances with extraordinary rates and near perfect efficiencies in spite of their site. This is not the case if the peptide is in water, where the efficiency of charge hopping to the next site is reduced to approximately 2 %. Here, water is not an ideal solvent for charge transport. The issue at hand is how to explain such enormous charge transfer quenching in water compared to another typical medium, 10 lipids. We performed molecular dynamics simulations to computationally substantiate the novel long-distance charge transfer yield of the polypeptides in lipids. This is characterized by the charge transfer persistent-distance decay constant and not by the rate, which is seldom, if ever, measured and hence not directly addressed here. This model can encompass an extremely wide range of yields over very long distances in peptides in various media. The calculations here demonstrate the good charge 15 transport efficiency in lipids in contrast to the poor efficiency in water. The protein charge transport also exhibits a very strong anisotropic effect in lipids. The peptide secondary structure effect of charge transfer in membranes is analyzed in contrast to that in water. These results suggest that this model can be useful for the prediction of charge transfer efficiency in various environments of interest and indicate that the charge transfer is highly efficient in membrane proteins.

20

Abbreviations:

DPPC: Dipalmitoylphosphatidylcholine, DMPC: Dimyristoylphosphatidylcholine, T_c: Phase Transition Temperature, MD: Molecular Dynamics, FPTD: First Passage Time Distribution.

25

A   Introduction

Protein charge-transfer is a fundamental process in a variety of biological systems, such as respiration, photosynthesis and the nitrogen cycle.[1-5] This process strongly depends upon protein motion, which is inevitably influenced by the environment of the protein. Weinkauf et al.[6-9] revealed that for isolated short peptide chains, which are ionized at the C-terminus, the charge and reactivity travel on an extremely rapid time scale through each of the 6-8 residues to the N-terminus. Reactivity was only observed at the N-terminus. Gray et al.[10-12] showed that the electron transfer of the Ru-modified proteins, such as α-helix myoglobin and β-sheet azurin, in water is distance-dependent but of low efficiency. The experiments on short peptides showed that the charge transfer process in isolated molecules is very efficient, whereas the same process in water is approximately two orders of magnitude less efficient.[11-14] Hence, water is not an ideal solvent for charge transport. The transport inefficiency in water raises the interesting question of whether a lipid environment is friendlier for charge transfer, as many of these peptides are constituents of membrane proteins.

Membrane proteins, such as ion channels, ion pumps, cytochrome *c* oxidase, photosynthetic reaction centers, etc., are highly structurally and functionally diverse.[15-22] Typically, charge transfers are photo-induced or redox potential-driven; for example, photo-induced electron transfer occurs in the photosynthetic reaction center, and redox-driven electron transfer occurs in metalloproteins[23,24] and voltage-driven membrane proteins.[25] Electron transfer in membrane proteins has attracted extensive experimental and computational studies.[23,26-39] For example, time-resolved experiments show that the voltage changes in the redox-driven proton pump cytochrome *c* oxidase can induce electron transfer reactions within the enzyme.[26] DsbD-mediated electron transfer reactions are driven by multistep redox reactions and the electrons flow from cytoplasm thioredoxin to periplasmic substrates.[33-37] In quinol-nitrate oxidoreductase NarGHI, the electrons are transferred from the oxidation site of FdnGHI in the periplasm to the reduction site of NarGHI in the cytoplasm.[40-44] It is well known that the photosynthetic reaction center has a very high efficiency (> 90 %) of charge transfer and a fast rate (< 10^{-10} s^{-1}).[45]

We then interpret these widely varying environmental systems in terms of a bifunctional model[46] that uses a special ratchet and hopping model. The coupling between the amino acid sites in the bifunctional model requires a critical configuration of the adjacent carbonyl groups. These transition states are obtained by rotation of the Ramachandran angles. Molecular dynamics (MD) calculations show that the time required to obtain such critical configuration is 140 fs.[47]

Interestingly, this value completely agrees with recent 2D-IR measurements of a tripeptide carried out by Hamm.[48,49] Despite the fact that the time scale is found to be similar in water and in vacuum, the efficiency drops by two orders of magnitude. Hence, the difference between the mediums is not due to rates but due to efficiencies. Note that the dynamic motion of water is by far the fastest and includes librational (rotational) and diffusive motion with time scales of 126 fs and 880 fs,[50] respectively. The water molecular translation is longer; compared to the amino acid torsion motion, the molecular motion in water is relatively rigid.[50] In vacuum, the torsional mobility is assured; hence, the charge transport is very efficient. This indicates the innate facility of charge transport in an unencumbered peptide structure over a distance. If this motion is impeded either intramolecularly or by the environment, the charge transport yield is severely suppressed. Several studies have successfully supported this model for isolated polypeptide chains and similar molecules in water.[47,51-54] Nevertheless, the efficiency in a lipid system has not been studied, and the role of the warping membrane protein in charge transfer is still unclear. Herein, we predict that this bifunctional model could be improved in certain lipid systems.

Previous work has explored membrane participation in many vital transport processes in biological systems. From a fundamental point of view, the membrane has a pseudo-phase transition close to room temperature because of the tilt change of the lipid chain axis. Lipids have two inherent properties different from those of water: the dielectric constant and the pseudo-phase transition. The dielectric constant of water is approximately 80, but it is 2-10 for the alkyl region of the lipids, which is quite different from that of the water system. For example, dipalmitoylphosphatidylcholine (DPPC) and dimyristoylphosphatidylcholine (DMPC) are among the most widely used lipids in computation. The fluid-to-gel phase transition temperatures T_c for DPPC and DMPC are 303 K and 296 K, respectively.[55,56] Above the phase transition temperature T_c, lipid molecules are free to rotate and turn in a fluid structure with a more random configuration. On the contrary, below T_c, the motion of the lipid molecule is slow and the lipid bilayer forms a gel-like structure.

In the present study, we pursue the bifunctional model to investigate the effect of a lipid environment on the peptide charge transfer by using local heating MD simulation. Our results show that when the principal axis of an embedded peptide is orthogonal to the lipid chain, there is no charge transfer. When the peptide aligns with the lipid chain, the charge transfer efficiency becomes very high and is even higher than in vacuum or in water. This appears to warrant two conclusions: (1) charge conductivity of the peptide in a membrane environment is highly anisotropic; and (2) the

membrane greatly enhances the charge transfer efficiency and thus becomes an important environment of choice in charge transfer that is far more preferable than water.

B Theory

5 **Bifunctional model.** It has been shown that the bifunctional model can successfully explore charge transfer in a polypeptide chain.[47] This model describes the charge transport from the C-terminus to the N-terminus along a polypeptide chain involving two coupling regimes at Ramachandran angles (φ, ψ) (Fig. 1). The coupling between the amino acid sites requires a critical configuration of the neighboring carbonyl groups with energy degeneracy,[46,57] where the O and O atoms of the carbonyl

10 groups on the adjacent amino acids come close to the critical distance $d_{o-o,c}$ = 2.8 Å. This is also called a rest and fire mechanism. Intriguingly, the charge transition occurs in femtoseconds.

A direct timing measurement has shown the electronic energy jump between the neighboring amino acids ranging from 0.07 eV to 0.5 eV.[8] *Ab initio* computations[46] show that even a pair of two identical amino acids will have an ionization energy asymmetry of 0.6 eV due to the natural

15 asymmetry of the C-side and the N-side of each amino acid. For the ionic species in a small range of φ and ψ, the electronic energy degeneracy approaches a minimum. From a symmetric perspective, an isoenergetic state exists in both carbonyl groups, where the two states are strongly correlated and form one hybridized state. The successful "charge transfer" is counted as the adjacent carbonyl groups collision. Accordingly, the transition probability is denoted as the yield, i.e., successful

20 charge hopping, in mass spectroscopy. Hence, the charge transfer is determined in terms of efficiency instead of rate.

L-efficiency and decay constant (β-value). A peptide can be modeled as a sequence of residues on a string. At the residue juncture, we assume a rate constant for the charge transfer, k_t, and a rate constant for loss to the bath, k_b. The fraction that continues on in charge transfer is thus

25 $a = k_t /(k_t + k_b)$, referring to the local efficiency (L-efficiency); after n residues, the survival fraction of the charge is a^n. Because the typical inter-residue distance is 3.7 Å per unit, the full length of the chain is $R = 3.7\,n$. Thus, by expressing in exponential form $e^{n \ln a} = e^{-\beta R}$ ($a^n = e^{n \ln a}$), the following is given

$$\beta\text{-value} = -\frac{\ln a}{3.7}.$$ (1)

where the β-value is the distance-dependent decay constant of charge transfer in unit of Å^{-1}. Here, our simple model connects the β-value and the L-efficiency.

The β-value was obtained based on classical mechanics without considering the super-exchange model.[58] For example, for a rapid decay process, one obtains a large β-value. If the primary structure of peptide chain is homogeneous, the *a*-value is constant and the L-efficiency of all the residues is the same. On the other hand, if it is heterogeneous, the *a*-value is no longer a constant in equation (1) and the L-efficiency at each site is different. Therefore, the relationship of the *a*-value and the β-value in the electron transfer of a heterogeneous peptide becomes more complicated. Moreover, we also have to consider the influences of the protein dynamics and the solvent dynamics on the β-value that are usually not considered in electron transfer theory. Notably, our bifunctional model takes these effects directly into account.

Local heating: Molecular dynamics simulation. The typical C=O….O=C distance (d_{O-O}) between two nearby amino acids of a helical protein is approximately 3.8 Å. A local heating MD simulation is adopted to carry out the torsion motion inside the Ramachandran plot. A certain amount of the rotational energy is provided to a specified site with a local heating energy, E_{k_BT}, where the energy is in units of thermal energy, k_B is the Boltzmann constant and T is temperature. This heating energy is initially introduced to the rotational degrees of freedom of the $\overrightarrow{C_\alpha C}$ axis at the C-side of the C_α-hinge of the chosen residue. In fact, the rotational energy is propagated along the peptide chain with a shorter time scale (~100 fs), until it is scattered by the phonons. The evidence that this model produces far slower results was confirmed by Lifshitz in dipeptides.[59] Eventually, the vibrational modes dissipate the heat energy with a longer time scale (~ 1.0 ps) and the charge transport efficiency decays gradually.
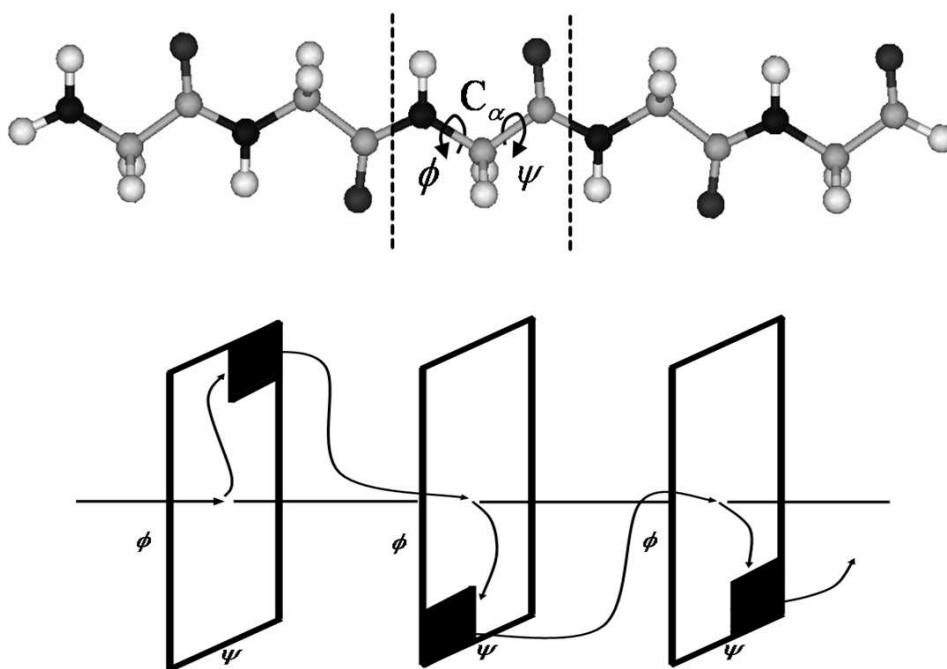
Fig. 1 Mechanism for charge transfer along a polypeptide chain from the C-terminus to the N-terminus. At each C_α-atom, there are two torsion angles, ψ and φ. This constitutes the so-called Ramachandran plot for each amino acid (upper part). In the lower part, we show that the torsion motions of ψ and φ correspond to a trajectory inside the Ramachandran plot phase space. One can picture a pseudo particle moving inside the box but with a specific angle as a gate for this particle to escape. Once this particle escapes out of the gate, it hops to the nearby Ramachandran plot or box and continues the same process until it reaches the N-terminus.

In addition to the local heating site, the temperature of rest is kept at the background temperature. The transition probability for a successful charge transfer between two nearby amino acids can be calculated by

$$\text{L-efficiency} = \frac{(\text{the successful configurations of the C=O .... O=C collisions})}{(\text{total configurations})} \qquad (2)$$

where the successful configuration of the C=O….O=C collisions is counted at $d_{o-o} = d_{o-o,c}$. Only a fraction of configurations fulfills the transition and leads to the L-efficiency being less than unit. We are able to calculate the first passage time distribution (FPTD) of the C=O….O=C collision, in which the energy dissipation time can be obtained and the mean value is reflected at the peak position of the FPTD. Furthermore, the global efficiency (G-efficiency) can be obtained by taking

the product of L_y^x, where x is the local heating site and L_y denotes the L-efficiency at the y residue. Thus, the G-efficiency is fitted by $Ae^{-\beta R}$ and the β-value can be extracted from

$$\text{G-efficiency} = \prod_{y=donor}^{acceptor} L_y^x = Ae^{-\beta R} \tag{3}$$

where the G-efficiency characterizes the global efficiency of charge transfer from the donor to the acceptor along the polypeptide chain, A is a pre-factor, and the β-value quantifies the persistence length of the charge transfer.[51] For instance, one might have a high L-efficiency and a large β-value (small G-efficiency) due to a quick dump of the energy into the heat bath; in contrast, a small β-value (large G-efficiency) indicates that the reactivity can persist over a distance.

C Computational details

All of the MD simulations were performed with the program CHARMM[60] and the CHARMM36 force field[61] with the TIP3P water model[62] in a box with the dimensions 60×60×100 Å^3. The van der Waals radius of O atom is 1.4 Å. We constructed the lipid bilayer structures with Roux's method.[63] A detailed procedure was described in our previous work.[53] The initial structures of two α-helical membrane proteins, KcsA a-chain and melittin, were taken from the Protein Databank using accession codes 1bl8 and 2mlt, respectively; then, energy minimization was conducted. A parallel membrane protein system was built by inserting the minimized KcsA a-chain into a 90 DPPC lipid bilayer (Fig. 2a), and the orthogonal system comprised the melittin embedded in a DMPC lipid bilayer (Fig. 2b). Furthermore, each system was subjected to energy minimization, heating, and 100 ns equilibration. More than 3000 configurations were generated for analysis by performing local heating MD simulations. The SHAKE algorithm[64] was applied to constrain the bonds involving hydrogen atoms and the non-bonding interaction was truncated at 12 Å. All the detailed local heating procedure was described in our previous work.[51] The local heating energy was provided to the local site with a corresponding temperature of 2667 K (~ 0.23 eV). We choose the local heating residue arbitrarily, but it should not be close to the boundary of the polypeptide chain to prevent the boundary effect. MD simulations were performed at four background temperatures: 200 and 250 K (below T_c,) and 310 and 350 K (above T_c,).
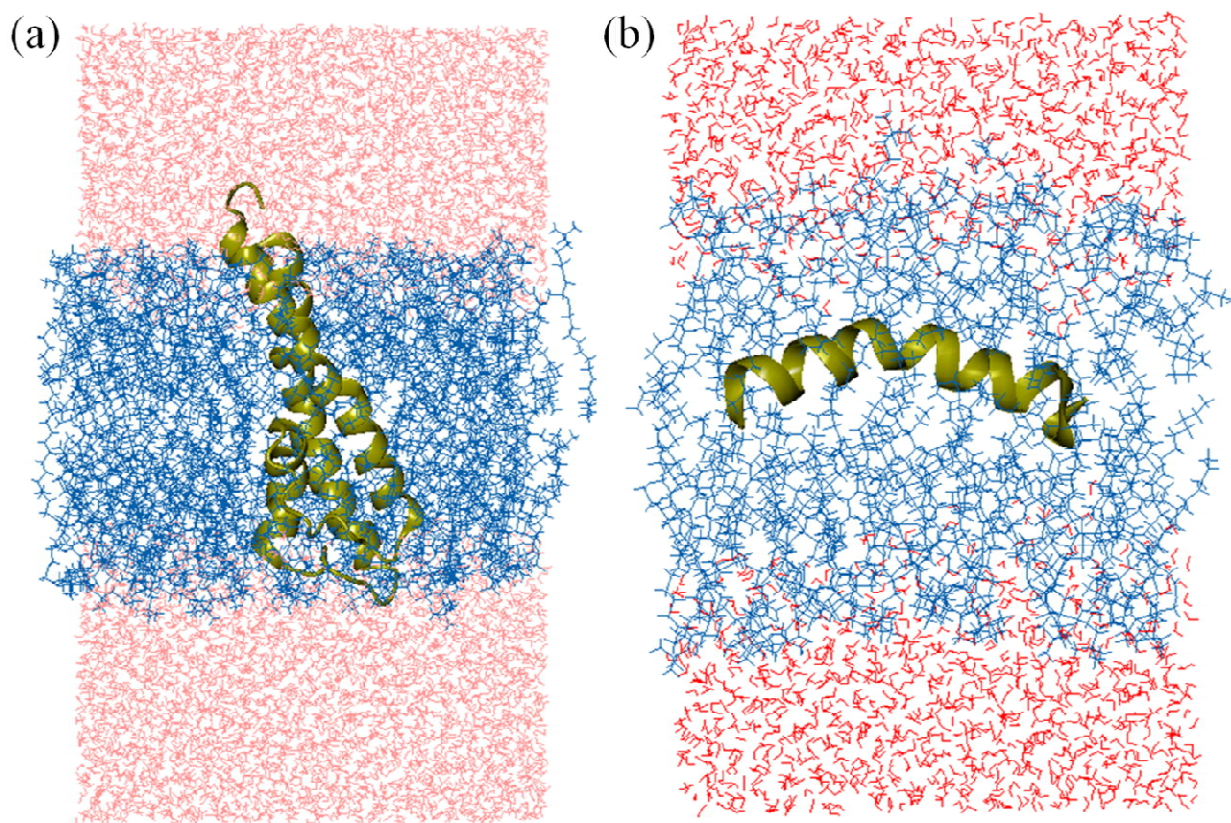
Fig. 2 Structures of the membrane proteins. (a) KcsA a-chain is parallel to the lipid layer. (b) Melittin is orthogonal to the lipid layer. The peptides are represented by the secondary rendering and colored yellow. The membrane and water molecules are colored blue and red, respectively.

D   Results and discussion

Lipid-phase effect. Lipids have two typical phases: a fluid-like phase and a gel-like phase. In the fluid-like phase ($T > T_c$), the lipid molecules move more freely than in the gel-like phase ($T < T_c$). It would be quite interesting to know whether the peptide charge transfer is dependent on the lipid phase transition. We have shown that a first-order lipid phase transition was accurately calculated by our previous MD simulations.[53] Therefore, it is appropriate to apply this method to investigate effect of the lipid phase transition on the peptide charge transfer.

We adopt one α-helix from the ion channel KcsA a-chain embedded in DPPC membrane system (Fig. 2a) to perform the local heating MD simulation. The local heating sites are Leu_{83} and Thr_{85}, separately. We display the L-efficiencies at each site in Fig. 3. Other efficiencies are

relatively small and are not shown. Comparing Figs. 3a and 3b, the L-efficiency drops abruptly until the fourth site away from the local heating site. Hence, the L-efficiency drop is independent of the type of residue. According to equation (3), the G-efficiency ratio of these two different local heating site situations gives a β-value. Across the phase transition temperature, the result exhibits an abrupt change in the L-efficiency at the local heating site and the L-efficiency decreases when the background temperature is increased. Remarkably, both the L-efficiency and β-value are somewhat smaller in the fluid-like phase than in the gel-like phase (Table 1). The trend of the L-efficiency drop supports the argument that in the fluid-like phase, the motion of the lipid molecule is fast so that the high collision frequency between the peptide and the lipid enhances the random motion of the C=O groups and the rotational energy is eventually dissipated to vibrational modes or thermal motion. However, below T_c, the peptide-lipid collision frequency is low, where the L-efficiency is slightly higher than that above T_c. Due to the tilt and rigid structure of the lipid molecules blocking the rotational motion of the peptide and throttling the charge transfer over a distance in the gel-like phase, we found a slightly larger β-value compared to that in the fluid-like phase. Obviously, the L-efficiency depends on the lipid phase transition.
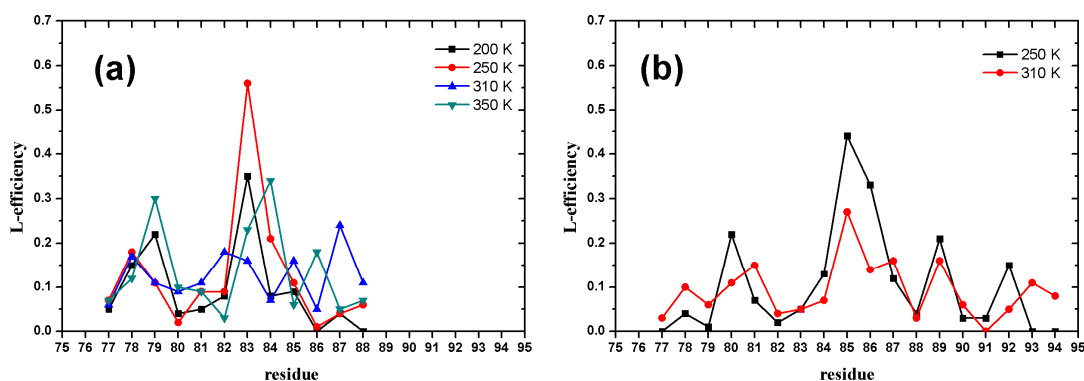

Fig. 3   Efficiency of each site for the parallel KcsA-A chain in the membrane. The local heating site is (a) Leu$_{83}$ and (b) Thr$_{85}$. The local heating energy is 2667 K. The background temperatures are 350, 310, 250 and 200 K.

Furthermore, the FPTD of the d_{o-o} close to 2.8 Å versus the background temperature is shown in Fig. 4. When T is above T_c, the FPTD is broad and decays slowly with a long time tail (Figs. 4a and 4b). At $T < T_c$, it decays more steeply (Figs. 4c and 4d). The L-efficiency is clearly reflected in

the sparsity of points and the noise in the FPTD. Because the lipid reaction field and the peptide-lipid interactions are weak, the energy dissipation is less during the collision process. The intra-peptide hydrogen bond could also be reduced by the lipid reaction field, whereas the intra-peptide hydrogen bond energy above T_c is slightly lower than T_c.[53] The reduction of the hydrogen bond strength in lipid is attributed to the dynamic similarity with the lipid medium. Therefore, the possibility of the C=O…O=C collision still exists even at the long time.

In principle, the carbonyl group rotational fluctuation and the collision time scale correspond to the standard deviation σ and the mean value μ of the FPTD, respectively. We obtain

$$\sigma^2 = \int_0^\infty dt (FPTD(t) - \mu)^2 ,$$ where σ is the width at the half-height of the FPTD and t is the time.

Based on Fig. 4, the μ and σ values are estimated about: (164, 436) at 350 K, (152, 267) at 310 K, (120, 73) at 250 K, and (115, 73) at 200 K, and the values are in unit of fs. We find that both μ and σ values increase as the background temperature increases. This clarifies that in the gel-like phase, the peptide-lipid collision frequency is low and the rotational fluctuation is depressed. In this scenario, the peptide motion is similar to that of an isolated molecule, and the μ value is smaller. However, in the fluid-like phase, the motion of the lipid molecule is fast enough to obstruct the carbonyl group to rotate freely, and one obtains a high μ value. Hence, the fluid-like phase could promote charge transfer over a longer distance with high efficiency, even better than would the gel-like phase. This observation strongly supports the lipid-phase effect on protein charge-transfer.

Table 1. The β-value of the peptide in various media.

Peptide (medium)	β-value	
	experimental data (Å^{-1})	bifunctional model (Å^{-1})
α-helix (water) (vacuum)	1.3	1.31 1.16
β-sheet (water)	1.0	1.0
α-helix (DPPC) $T > T_c$ (T = 310 K) $T < T_c$ (T = 250 K)		0.79 0.84
β-sheet (DPPC) $T > T_c$ (T = 310 K) $T < T_c$ (T = 250 K)		0.92* 0.94*

* The β-value of the β-sheet peptide is calculated using a geometric sum, which is based on the assumption of the azurin consisting of three linear chains. We followed the same method adopted in our previous paper,[51] i.e., β-value of β-sheet = (β-value of α-helix)$^{1/3}$.
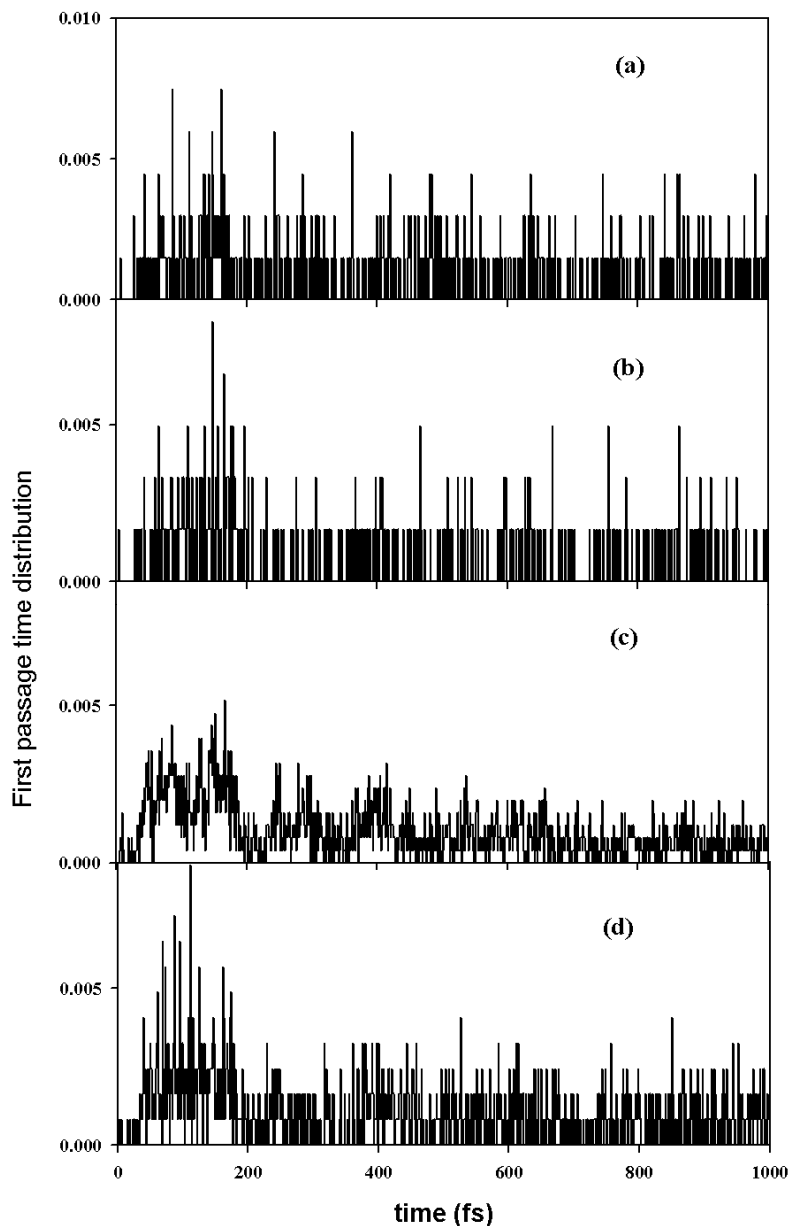
Fig. 4 The FPTD vs. time at the local heating site Leu_{83} with the energy 2667 K. The systems correspond to the background temperatures: (a) 350 K, (b) 310 K, (c) 250 K, and (d) 200 K. The distribution is normalized with the successful configuration of the C=O….O=C collision.

5

Medium effect. Our previous studies have shown a near unit of the L-efficiency for an isolated peptide.[51] However, for an α-helix in lipids, one obtains a smaller L-efficiency than in vacuum (Fig. 3). Our results show that the L-efficiency at the local heating site in the medium follows the order ~1.0 (in vacuum)[51] > ~ 0.3 − 0.6 (in lipid) ≥ ~ 0.4 (in water).[52] This is due to the reaction field

effect. The dielectric constant of lipids is approximately 2-10 times higher than that of vacuum. Because the reaction field effect of lipids is much weaker than that of water, the strength of the intra-peptide hydrogen bond in lipids is stronger than in water.[53] The hydrogen bond flexibility in the medium follows the order water > lipid > vacuum. In comparison, for an isolated peptide, the intra-peptide hydrogen bond is more rigid and hinders the C=O…O=C collision, so there is a high intensity peak of the L-efficiency at the local heating site. In water, the water barrel surrounding the peptide is expected to seriously impede the C=O…O=C collision, having a μ value of approximately 190 fs.[52] In vacuum and in water systems, the FPTD long time tail is almost absent before the vibration modes turn up. Hence, the solvent effect depresses the occurrence of the carbonyl group collisions.

Interestingly, in the KcsA a-chain membrane system, the peptide retains its native structure due to the weak peptide-lipid interaction; thereby, its local heating energy could be effectively transferred over a longer distance and has a high G-efficiency. Our results show that the β-value follows the order 0.79 – 0.84 (in lipid) < 1.16 (in vacuum)[51] < 1.31 (in water)[52] (see Table 1). These findings highlight that lipids could be an excellent medium for peptide charge transport.

Peptide-lipid orientation effect. Moreover, we consider whether the protein charge-transfer in lipids depends on the relative peptide-lipid orientation. Here, two systems are built: the parallel KcsA (Fig. 2a) and the orthogonal melittin (Fig. 2b) in lipids. The results show that there is no charge transfer in the orthogonal system. However, the charge transfer in the parallel system is highly efficient with a small β-value, which is even smaller than in vacuum and in water (Table 1). In the orthogonal system, the lipid tail structure could block the peptide motion no matter whether it is in the fluid-like phase or in the gel-like phase. For the parallel system, the influence of the charge transfer efficiency was discussed in the preceding section. This constitutes a most interesting anisotropy for a peptide charge transfer in a lipid system and again demonstrates that protein motions are required for charge transport.

Secondary structure effect. For an α-helical KcsA a-chain in lipid, the β-values at 250 K ($< T_c$) and 310 K ($> T_c$) are 0.84 and 0.79 Å^{-1}, respectively (Table 1). In comparison with the β-sheet in the same phase, the α-helix always has a somewhat smaller β-value, implying that the charge transfer efficiency of the α-helix is superior to that of the β-sheet in lipids. However, the β-sheet has slightly higher efficiency than the α-helix in water. This is because the intra-peptide hydrogen bond strength of the β-sheet is about two times stronger in lipids than that in water and the number of hydrogen

bonds is not reduced, as they are in water.[65] Thus, there is a strong solvent effect on the strength of the hydrogen bond. The solvent effect differs considerably depending on the protein secondary structure. It explicitly confirms that the secondary protein structure effect on the charge transfer in lipids contrasts that observed in water.

E Conclusion

Polypeptide chains in membranes show a new distal reaction scheme. Charge transfer along polypeptide chains can be generally described by a distance-dependent decay constant β-value. For the gas phase, we have discovered a highly efficient and extremely fast long-distance transport of charge and reactivity, a process unique to polypeptides and not found in typical molecules. Such a rapid charge and energy transfer outruns statistical distributions of vibrational degrees of freedom, such as in any RRKM theory. The charge transfer yield was throttled by two orders of magnitude in water because the slow-moving water medium on the outside of the peptide interferes with the very fast dihedral motions of the peptide — on this timescale, the water acts as an iceberg.[50,66] In our model, lipids are again seen to constitute a very different environment. Most interestingly, our calculations even predict phase transitions in the lipid with excellent accuracy. The peptide charge transport is again observed to be highly efficient in lipids, particularly in certain orientations and phases. This constitutes a third environment for our model of very rapid charge transport in proteins, a process open to new dimensions due to these environmental factors. These results highlight an excellent persistence of charge transfer in a membrane environment, even better than in vacuum and certainly much better than in water. Hence, lipids are an excellent medium for charge and reactive transport, as is perhaps expected. In this manner, the environment constitutes an additional important parameter influencing protein reactivity and engineering.

Notes

ᵃ Department of Life Sciences and Institute of Genome Sciences, and Institute of Biomedical Informatics, National Yang-Ming University, Taipei 112, Taiwan

ᵇ Institut für Physikalische und Theoretische Chemie, TU-München, Lichtenbergstr. 4, 85748
₅ *Garching, Germany*

ᶜ Institute of Atomic and Molecular Sciences, Academia Sinica, Taipei 106, Taiwan

*To whom correspondence should be addressed: Sheh-Yi Sheu, Fax: 886-2-28202449; Tel: 886-2-28267233; Email: sysheu@ym.edu.tw; Dah-Yen Yang, Fax: 886-2-23620200; Tel: 886-2-23668239; Email: dyyang@po.iams.sinica.edu.tw

₁₀ *The authors declare no conflict of interest.*

References:

1.   G. D. Scholes, G. R. Fleming, A. Olaya-Castro and R. van Grondelle, *Nat Chem*, 2011, **3**, 763-774.

₁₅ 2.   E. Rios, G. Pizarro and E. Stefani, *Annu. Rev. Physiol.*, 1992, **54**, 109-133.

3.   S. L. Mayo, W. R. Ellis, Jr., R. J. Crutchley and H. B. Gray, *Science*, 1986, **233**, 948-952.

4.   M. Hervás, J. A. Navarro and M. A. De la Rosa, *Acc. Chem. Res.*, 2003, **36**, 798-805.

5.   L. M. Utschig and M. C. Thurnauer, *Acc. Chem. Res.*, 2004, **37**, 439-447.

6.   R. Weinkauf, P. Schanen, A. Metsala and E. W. Schlag, *J. Phys. Chem.*, 1996, **100**, 18567-
₂₀   18585.

7.   R. Weinkauf, P. Aicher, G. Wesley, J. Grotemeyer and E. W. Schlag, *J. Phys. Chem.*, 1994, **98**, 8381-8391.

8.   R. Weinkauf, P. Schanen, D. Yang, S. Soukara and E. W. Schlag, *J. Phys. Chem.*, 1995, **99**, 11255-11265.

₂₅ 9.   R. Weinkauf, E. W. Schlag, T. J. Martinez and R. D. Levine, *J. Phys. Chem. A*, 1997, **101**, 7702-7710.

10.   R. Langen, I. J. Chang, J. P. Germanas, J. H. Richards, J. R. Winkler and H. B. Gray, *Science*, 1995, **268**, 1733-1735.

11.   J. R. Winkler and H. B. Gray, *J. Biol. Inorg. Chem.*, 1997, **2**, 399-404.

₃₀ 12.   A. Ponce, H. B. Gray and J. R. Winkler, *J. Am. Chem. Soc.*, 2000, **122**, 8187-8191.

13.   N. Borovok, A. B. Kotlyar, I. Pecht, L. K. Skov and O. Farver, *FEBS Lett.*, **457**, 277-282.

14. O. Farver, J. Zhang, Q. Chi, I. Pecht and J. Ulstrup, *Proc. Natl. Acad. Sci. U. S. A.*, 2001, **98**, 4426-4430.

15. S. S. Hasan, E. Yamashita and W. A. Cramer, *Biochim. Biophys. Acta - Bioenergetics*, 2013, **1827**, 1295-1308.

16. E. Gouaux and R. MacKinnon, *Science*, 2005, **310**, 1461-1465.

17. J. Deisenhofer, O. Epp, K. Miki, R. Huber and H. Michel, *Nature*, 1985, **318**, 618-624.

18. P. Navas, F. J. Alcain, I. Burón, J.-C. Rodríquez-Aguilera, J. M. Villalba, D. M. Morré and D. J. Morré, *FEBS Lett.*, 1992, **299**, 223-226.

19. E. J. Stewart, F. Katzen and J. Beckwith, *EMBO J.*, 1999, **18**, 5963-5971.

20. J. A. Lake, M. W. Clark, E. Henderson, S. P. Fay, M. Oakes, A. Scheinman, J. P. Thornber and R. A. Mah, *Proc. Natl. Acad. Sci. U. S. A.*, 1985, **82**, 3716-3720.

21. C. C. Moser, C. C. Page and P. L. Dutton, *Philos. trans. - R. Soc., Biol. sci.*, 2006, **361**, 1295-1305.

22. L. A. Sazanov, *Biochemistry*, 2007, **46**, 2275-2288.

23. J. J. Warren, N. Herrera, M. G. Hill, J. R. Winkler and H. B. Gray, *J. Am. Chem. Soc.*, 2013, **135**, 11151-11158.

24. H. B. Gray and J. R. Winkler, *Biochim. Biophys. Acta - Bioenergetics*, 2010, **1797**, 1563-1572.

25. J. P. Collman, N. K. Devaraj, R. A. Decréau, Y. Yang, Y.-L. Yan, W. Ebina, T. A. Eberspacher and C. E. D. Chidsey, *Science*, 2007, **315**, 1565-1568.

26. I. Belevich, D. A. Bloch, N. Belevich, M. Wikström and M. I. Verkhovsky, *Proc. Natl. Acad. Sci. U. S. A.*, 2007, **104**, 2685-2690.

27. P. Brzezinski, A. Messinger, Y. Blatt, A. Gopher and D. Kleinfeld, *J. Membr. Biol.*, 1998, **165**, 213-225.

28. A. Pilotelle-Bunner, P. Beaunier, J. Tandori, P. Maroti, R. J. Clarke and P. Sebban, *Biochim. Biophys. Acta - Bioenergetics*, 2009, **1787**, 1039-1049.

29. D. Alvarez-Paggi, U. Zitare and D. H. Murgida, *Biochim. Biophys. Acta - Bioenergetics*, 2014, **1837**, 1196-1207.

30. M. L. Cartron, J. D. Olsen, M. Sener, P. J. Jackson, A. A. Brindley, P. Qian, M. J. Dickman, G. J. Leggett, K. Schulten and C. Neil Hunter, *Biochim. Biophys. Acta - Bioenergetics*, 2014, **1837**, 1769-1780.

31. I. Kim, S. Chakrabarty, P. Brzezinski and A. Warshel, *Proc. Natl. Acad. Sci. U. S. A.*, 2014,

111, 11353-11358.

32. N. Nilsen, W. Brownell, S. Sun and A. Spector, *Biomech. Model. Mechanobiol.*, 2012, **11**, 107-118.

33. F. Katzen and J. Beckwith, *Cell*, 2000, **103**, 769-779.

34. A. Rozhkova and R. Glockshuber, *J. Mol. Biol.*, 2008, **380**, 783-788.

35. S.-H. Cho and J. Beckwith, *J. Biol. Chem.*, 2009, **284**, 11416-11424.

36. B. Heras, S. R. Shouldice, M. Totsika, M. J. Scanlon, M. A. Schembri and J. L. Martin, *Nat. Rev. Micro.*, 2009, **7**, 215-225.

37. S.-H. Cho, D. Parsonage, C. Thurston, R. J. Dutton, L. B. Poole, J.-F. Collet and J. Beckwith, *mBio*, 2012, **3**, e00291-00211.

38. P. Pospíšil, K. E. Luxem, M. Ener, J. Sýkora, J. Kocábová, H. B. Gray, A. Vlček and M. Hof, *J. Phys. Chem. B*, 2014, **118**, 10085-10091.

39. J. Henderson, S. D. Glover, B. J. Lear, D. Walker, J. R. Winkler, H. B. Gray and C. P. Kubiak, *J. Phys. Chem. B*, 2014.

40. M. G. Bertero, R. A. Rothery, M. Palak, C. Hou, D. Lim, F. Blasco, J. H. Weiner and N. C. J. Strynadka, *Nat. Struct. Mol. Biol.*, 2003, **10**, 681-687.

41. R. A. Rothery, M. G. Bertero, R. Cammack, M. Palak, F. Blasco, N. C. J. Strynadka and J. H. Weiner, *Biochemistry*, 2004, **43**, 5324-5333.

42. F. Blasco, B. Guigliarelli, A. Magalon, M. Asso, G. Giordano and R. A. Rothery, *Cell. Mol. Life Sci.*, 2001, **58**, 179-193.

43. G. Schwarz, R. R. Mendel and M. W. Ribbe, *Nature*, 2009, **460**, 839-847.

44. S. V. Antonyuk, C. Han, R. R. Eady and S. S. Hasnain, *Nature*, 2013, **496**, 123-126.

45. C. A. Wraight and R. K. Clayton, *Biochim. Biophys. Acta*, 1974, **333**, 246-260.

46. L. Y. Baranov and E. W. Schlag, *Z. Naturforsch., A: Phys. Sci.*, 1999, **54**, 387-396.

47. E. W. Schlag, S. Y. Sheu, D. Y. Yang, H. L. Selzle and S. H. Lin, *Proc. Natl. Acad. Sci. U. S. A.*, 2000, **97**, 1068-1072.

48. S. Woutersen and P. Hamm, *J. Phys. Chem. B*, 2000, **104**, 11316-11320.

49. S. Woutersen, Y. Mu, G. Stock and P. Hamm, *Proc. Natl. Acad. Sci. U. S. A.*, 2001, **98**, 11254-11258.

50. R. Jimenez, G. R. Fleming, P. V. Kumar and M. Maroncelli, *Nature*, 1994, **369**, 471-473.

51. S. Y. Sheu, E. W. Schlag, D. Y. Yang and H. L. Selzle, *J. Phys. Chem. A*, 2001, **105**, 6353-6361.

52. S. Y. Sheu, D. Y. Yang, H. L. Selzle and E. W. Schlag, *J. Phys. Chem. A*, 2002, **106**, 9390-9396.

53. S. Y. Sheu, E. W. Schlag, H. L. Selzle and D. Y. Yang, *J. Phys. Chem. B*, 2009, **113**, 5318-5326.

54. D. V. Vyalikh, V. V. Maslyuk, A. Blüher, A. Kade, K. Kummer, Y. S. Dedkov, T. Bredow, I. Mertig, M. Mertig and S. L. Molodtsov, *Phys. Rev. Lett.*, 2009, **102**, 98101.

55. C. H. Lee, W. C. Lin and J. Wang, *Phys. Rev. E*, 2001, **64**, 20901.

56. A. Taly, L. Baciou and P. Sebban, *FEBS Lett.*, 2002, **532**, 91-96.

57. L. Serrano-Andrés and M. P. Fülscher, *J. Phys. Chem. B*, 2001, **105**, 9323-9330.

58. D. N. Beratan, J. N. Onuchic and J. J. Hopfield, *J. Chem. Phys.*, 1987, **86**, 4488-4498.

59. Y. Hu, B. Hadas, M. Davidovitz, B. Balta and C. Lifshitz, *J. Phys. Chem. A*, 2003, **107**, 6507-6514.

60. B. R. Brooks, R. E. Bruccoleri, B. D. Olafson, D. J. States, S. Swaminathan and M. Karplus, *J. Comput. Chem.*, 1983, **4**, 187-217.

61. A. D. MacKerell, Jr, D. Bashford, M. Bellott, R. L. Dunbrack, Jr., J. D. Evanseck, M. J. Field, S. Fischer, J. Gao, H. Guo, S. Ha, D. Joseph-McCarthy, L. Kuchnir, K. Kuczera, F. T. K. Lau, C. Mattos, S. Michnick, T. Ngo, D. T. Nguyen, B. Prodhom, W. E. Reiher, III, B. Roux, M. Schlenkrich, J. C. Smith, R. Stote, J. Straub, M. Watanabe, J. Wiorkiewicz-Kuczera, D. Yin and M. Karplus, *J. Phys. Chem. B*, 1998, **102**, 3586-3616.

62. W. L. Jorgensen, J. Chandrasekhar, J. D. Madura, R. W. Impey and M. L. Klein, *J. Chem. Phys.*, 1983, **79**, 926-935.

63. S. Berneche, M. Nina and B. Roux, *Biophys. J.*, 1998, **75**, 1603-1618.

64. J.-P. Ryckaert, G. Ciccotti and H. J. C. Berendsen, *J. Comput. Phys.*, 1977, **23**, 327-341.

65. S. Y. Sheu, D. Y. Yang, H. L. Selzle and E. W. Schlag, *Proc. Natl. Acad. Sci. U. S. A.*, 2003, **100**, 12683-12687.

66. H. S. Frank and M. W. Evans, *J. Chem. Phys.*, 1945, **13**, 507-532.